

to a macroporous molecule is fractional but by using very small particle diameters it can be increased somewhat to enable a separation to take place. The small particle size results in an extremely high back-pressure, and so column lengths are greatly reduced.

In a move away from particles it has become possible to polymerize the monomer/porogen mixture within the column itself, generating the pore structure in much the same way as particles but resulting in a monolith structure – a rigid polymeric cylinder containing through pores as well as diffusive pores. Columns containing such structures are now commercially available.

See also: II/Chromatography: Liquid: Mechanisms: Ion Chromatography; Mechanisms: Reversed Phases; Mechanisms: Size Exclusion Chromatography. III/Carbohydrates: Liquid Chromatography.

Further Reading

Hashimoto T (1991) Macroporous synthetic hydrophilic resin-based packings for the separation of biopolymers. *Journal of Chromatography* 544: 249–255.

Lloyd LL (1991) Rigid macroporous copolymers as stationary phases in high-performance liquid chromatography. *Journal of Chromatography* 544: 201–277.

Meehan E (1995) Semirigid polymer gels for size exclusion. In: Chi-san Wu (ed.) *Handbook of Size Exclusion Chromatography*, p. 25–46. New York: Marcel Dekker.

Moore JC (1964) Gel permeation chromatography. 1. A new method for molecular weight distribution of high polymers. *Journal of Polymer Science A* 2: 835–843.

Porath J and Flodin P (1959) Gel filtration: a method for desalting and group separation. *Nature* 183: 1657–1659.

Yang Y-B and Regnier FE (1991) Coated hydrophilic polystyrene-based packing materials. *Journal of Chromatography* 544: 233–247.

Yau WW, Ginnard CR and Kirkland JJ (1978) Broad-range linear calibration in high-performance size-exclusion chromatography using column packings with bimodal pores. *Journal of Chromatography* 149: 465–487.

Yau WW, Kirkland JJ and Bly DD (1979) Bimodal pore-size separations: optimum linearity and range. In: *Modern Size Exclusion Chromatography*, p. 267. New York: Wiley.

PORPHYRINS: LIQUID CHROMATOGRAPHY



C. K. Lim, MRC Toxicology Units, Leicester, UK

Copyright © 2000 Academic Press

Introduction

Porphyrins are cyclic tetrapyrrolic compounds (Figure 1) occurring widely in nature. They are, except for protoporphyrin, the oxidized by-product of the porphyrinogens (hexahydroporphyrins) which are the intermediates in the pathways of haem and chlorophyll biosynthesis.

The analysis and separation of porphyrins not only is important in the fields of chemistry and biochemistry of this important group of tetrapyrrolic pigments but is also valuable in the biochemical diagnosis of human porphyrias, a group of diseases associated with abnormal haem biosynthesis and consequently the overproduction of haem precursors. Since some of the enzymes of the haem pathway are sensitive to certain toxic chemicals, analysis of porphyrin excretion patterns may provide a sensitive indicator of exposure to these toxic chemicals which often results in characteristic and diagnostic metabolic alterations of the pathway.

Figure 2 shows the structures of some of the most commonly analysed naturally occurring porphyrins. High performance liquid chromatography (HPLC) is the best technique for the separation of these and other porphyrins. The resolution achieved by HPLC is far superior to other methods, including thin-layer chromatography and capillary electrophoresis (CE).

The HPLC separation of porphyrins, their important metal complexes and hexahydroporphyrins (por-

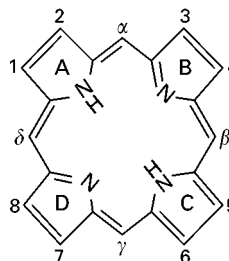


Figure 1 Structure of porphyrin macrocycle (Fischer's numbering system). The four pyrrole rings are designated A, B, C and D. The β -positions, which are usually substituted with acetic acid (Ac), propionic acid (Pr), methyl (Me), ethyl (Et) and vinyl (V) groups, are numbered 1–8. The four methine bridges or meso-positions are denoted α , β , γ and δ .

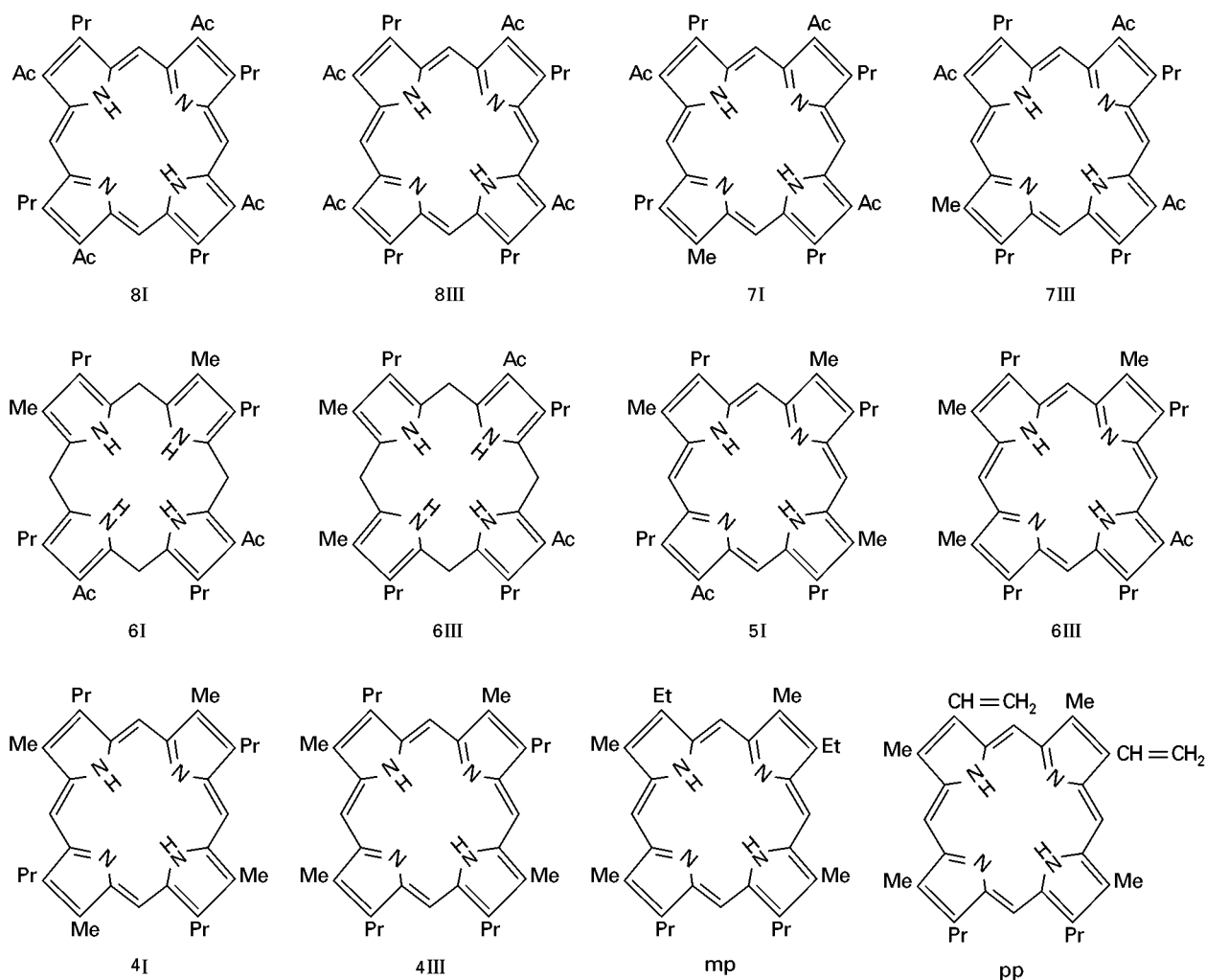


Figure 2 Structures of some commonly analysed naturally occurring porphyrins. 8I, Uroporphyrin I; 8III, uroporphyrin III; 7I, heptacarboxyl porphyrin I; 7III, heptacarboxyl porphyrin III; 6I, hexacarboxyl porphyrin I; 6III, hexacarboxyl porphyrin III; 5I, pentacarboxyl porphyrin I; 5III, pentacarboxyl porphyrin III; 4I, coproporphyrin I; 4III, coproporphyrin III; mp, mesoporphyrin; pp, protoporphyrin.

phyrinogens) are described below with particular reference to the choice of columns, mobile phases and methods of detection.

Separation of Porphyrin Methyl Esters

Porphyrins may be separated as the underivatized free acids or as their methyl esters following esterification of the carboxylic acid groups. The choice often depends on the application and the sample matrix in which the porphyrins are extracted.

Although many of the methods reported for the separation of porphyrin methyl esters are by normal-phase chromatography on silica, they are better separated by reversed-phase HPLC. Reversed-phase HPLC provides better resolution and is able to separate the type-I and type-III isomers of hexacarboxyl porphyrin hexamethyl ester, pentacarboxyl porphyrin pentamethyl ester and coproporphyrin tet-

ramethyl ester. Furthermore, the polar porphyrins (e.g. hydroxylated uroporphyrins) which are difficult to elute from normal-phase columns are easily eluted before uroporphyrin from the reversed-phase column because the elution order is the opposite of that encountered in normal-phase chromatography.

Figure 3 shows the separation of a mixture of porphyrin methyl esters by normal phase (A) and reversed-phase HPLC (B). The superiority of the latter is clearly demonstrated. The resolution of normal-phase separation could be improved by using 3- μ m particle size silica, but is still insufficient compared with RP-HPLC.

Separation of Porphyrin Free Acids

Choice of Column

Porphyrin free acids are best chromatographed on a reversed-phase column. Chemically bonded silica

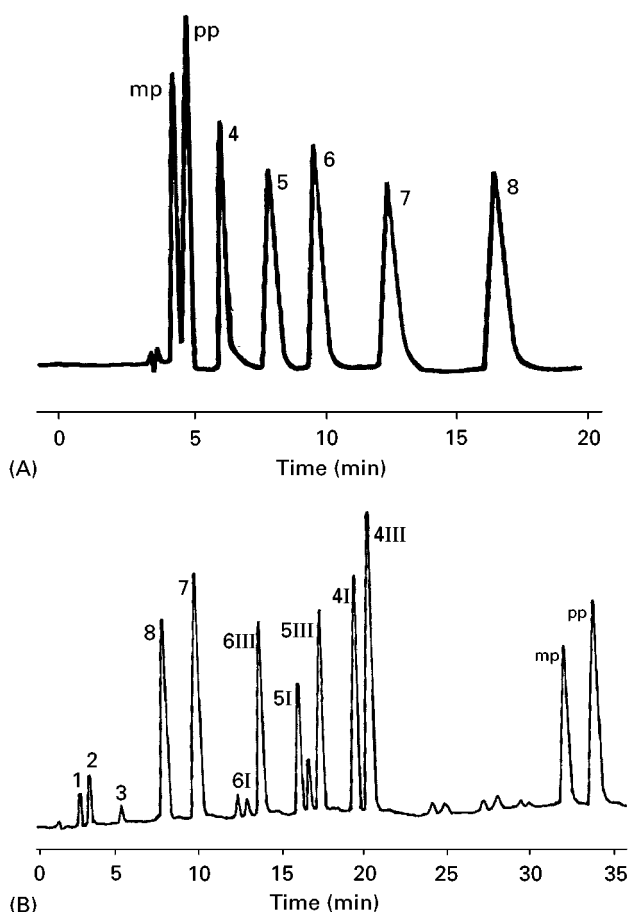


Figure 3 HPLC separation of porphyrin methyl esters. (A) Normal phase (μ Porasil, 300×4 mm, $10\text{-}\mu\text{m}$ particle size); eluent, n-heptane–methyl acetate (3 : 2, v/v); flow rate, 1.5 mL min^{-1} . (B) Reversed-phase (Hypersil ODS, 250×4.6 mm, $5\text{-}\mu\text{m}$ particle size); eluent, linear gradient elution from 70% acetonitrile in water to 100% acetonitrile in 30 min; flow rate, 1 mL min^{-1} . Peaks: 1, 2 and 3 = hydroxylated porphyrins; 4, 5, 6, 7 and 8 refer, respectively, to tetra- (copro), penta-, hexa-, hepta-, and octa- (uro) carboxyl porphyrin; I and III denote type-I and type-III isomers; mp = mesoporphyrin; pp = protoporphyrin.

with different hydrocarbon chain lengths, from C_1 (trimethylsilyl groups) to C_{18} (octadecylsilyl groups) have all been successfully used for the separation of porphyrins. A C_{18} column is preferred because it is more stable towards aqueous buffer than a C_1 column. The wide range of base-deactivated C_{18} column packings (e.g. Hypersil-BDS) further improves the efficiency of porphyrin separations and is the column of choice.

Choice of Mobile Phase

The porphyrins derived from the haem biosynthetic pathway are amphoteric compounds ionizable and soluble in both acids and bases. They are therefore

ideal for separation by RP-HPLC in the presence of an ion-pairing agent (e.g. tetrabutylammonium phosphate) or by ionization control with an acid (e.g. trifluoroacetic acid), a base (e.g. triethylamine) or a buffer solution (e.g. ammonium acetate buffer).

The choice of a correct mobile phase is obviously important for achieving an optimal separation. With the increasing use of online HPLC–mass spectrometry (LC–MS), the chosen mobile phase ideally should also be fully compatible with mass spectrometry. The introduction of hybrid electrospray quadrupole/time-of-flight MS allows sensitive and specific analysis of porphyrin free acids by LC–MS. To exploit this capability a mobile phase that is sufficiently volatile and is able to separate the whole range of porphyrins, including the complex type-isomers, is highly desirable. This rules out reversed-phase ion pair chromatography and the use of phosphate buffer. Simple acidic eluent such as 0.1% trifluoroacetic acid–acetonitrile mixtures can be used for the separation of porphyrins. However, resolution of the type-isomers of uro- and hepta-carboxyl porphyrins was not achieved although type-isomers of porphyrins with 6, 5, and 4 carboxyl groups were well separated.

To date, mobile phases containing ammonium acetate buffer provide excellent resolution and column efficiency as well as being fully compatible with

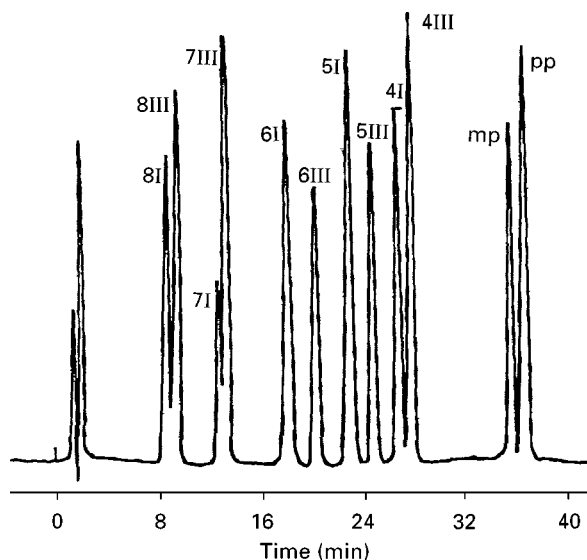


Figure 4 Separation of a standard mixture of porphyrins. Column, Hypersil-SAS (150×5 mm, $5\text{-}\mu\text{m}$ particle size); solvent A, 10% (v/v) acetonitrile in 1 M ammonium acetate buffer, pH 5.16; solvent B, 10% (v/v) acetonitrile in methanol; elution, 30 min linear gradient from 0% B to 65% B followed by isocratic elution at 65% B for a further 10 min; flow rate, 1 mL min^{-1} ; detection, 404 nm. Peaks: 8, 7, 6, 5 and 4 refer, respectively, to octa- (uro), hepta-, hexa-, penta- and tetra- (copro) carboxyl porphyrin; I and III denote type-I and type-III isomers; mp = mesoporphyrin; pp = protoporphyrin.

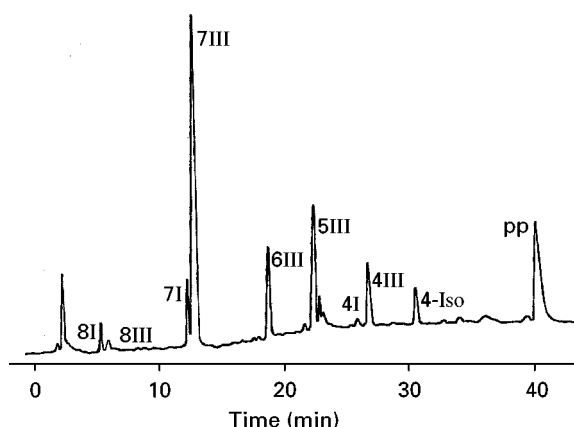


Figure 5 Separation of porphyrins in the faecal extract of a patient with porphyria cutanea tarda (PCT). Column, Hypersil-ODS (250×4.6 mm, $5\text{-}\mu\text{m}$ particle size); solvent A, 10% acetonitrile in 1 M ammonium acetate buffer (pH 5.16); solvent B, 10% acetonitrile in methanol; elution, linear gradient at 1 mL min^{-1} from 10% to 90% solvent B in 30 min, followed by isocratic elution at 90% B for a further 10 min; detection, 404 nm. Peaks: 4-Iso = isocoproporphyrin; pp = protoporphyrin; other peaks are identified as in Figures 3 and 4.

LC-MS operation. This buffer has been studied for the separation of porphyrins in detail and the following conclusions have been drawn:

1. The molar concentration of ammonium acetate buffer in the mobile phase significantly affected the retention and resolution. The optimum buffer concentration is 1 M. Below 0.5 M, excessive retention and peak broadening results, particularly in isocratic elution. At above 1.5 M, rapid elution with the consequent loss of resolution was observed.
2. The retention and resolution of the porphyrins are greatly influenced by the pH of the ammonium acetate buffer. Increasing the pH decreased the retention with loss of resolution. The optimum pH range is between 5.1 and 5.2, although this is column dependent. This pH range is, however, suitable for most reversed-phase columns.

In earlier studies it was shown that the isocratic elution of uroporphyrin I and III from reversed-phase columns was organic modifier specific and, with methanol as the organic modifier and 1 M ammonium acetate (pH 5.16) as the aqueous buffer, excessive retention and peak broadening was observed. The methanol adsorbed on the hydrocarbonaceous stationary phase surface is able to form extensive hydrogen bonds with the eight carboxyl groups of uroporphyrin, thus resulting in long retention and peak broadening. This effect is less significant in the separation of porphyrins with fewer

carboxyl groups. Nevertheless it is best to avoid using methanol as the sole organic modifier in porphyrin separations, especially when uroporphyrin is one of the components to be separated.

Replacing methanol with acetonitrile results in excellent resolution of uroporphyrin isomers within convenient retention times. Acetonitrile, however, is immiscible with 1 M ammonium acetate when its proportion is above 35% in the mobile phase. While acetonitrile-1 M ammonium acetate buffer mobile phase systems are excellent for the separation of porphyrins that can be eluted at up to 30% acetonitrile content (8-, 7-, 6-, 5- and 4-carboxyl porphyrins), they are not suitable for the separation of porphyrins that required a higher proportion of acetonitrile for elution, such as the dicarboxyl mesoporphyrin and protoporphyrin. In order to achieve simultaneous separation of all the porphyrins, therefore, a mixture of acetonitrile and methanol as the organic modifier is required. 1 M ammonium acetate buffer is completely miscible with methanol. A mixture consisting of 9–10% (v/v) acetonitrile in methanol as the organic modifier thus overcomes the hydrogen bonding effect caused by methanol and the solubility problem of 1 M ammonium acetate in acetonitrile. In practice, gradient

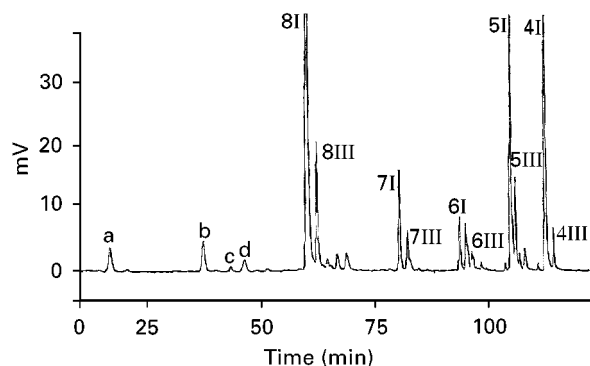


Figure 6 Separation of porphyrins in the urine of a patient with congenital erythropoietic porphyria (CEP). Column, Hypersil-BDS C_{18} (250×4.6 mm, $5\text{-}\mu\text{m}$ particle size); solvent A, 10% (v/v) acetonitrile in 1 M ammonium acetate buffer, pH 5.16; solvent B, 10% acetonitrile in methanol. The elution programme was: 0 to 20 min, isocratic elution at 100% A; 20 to 36 min, linear gradient from 0% B (100% A) to 8% B; 36 to 46 min, isocratic elution at 8% B; 46 to 56 min, linear gradient from 8% B to 16% B; 56 to 66 min, isocratic elution at 16% B; 66 to 86 min, linear gradient from 16% B to 30% B; 86 to 95 min, linear gradient from 30% B to 38% B; 95 to 108 min, linear gradient from 38% B to 42% B; 108 to 118 min, linear gradient from 42% B to 66% B; 118 to 128 min, linear gradient from 66% B to 75% B; 128 to 138 min, linear gradient from 75% B to 90% B; 138 to 145 min, isocratic elution at 90% B. The flow rate was 1 mL min^{-1} throughout. Detection, 404 nm. Peaks: a = meso-hydroxyuroporphyrin I; b = β -hydroxy propionic acid uroporphyrin I; c = hydroxyacetic acid uroporphyrin I; d = peroxyacetic acid uroporphyrin I. The other peaks are identified as in Figures 3 and 4.

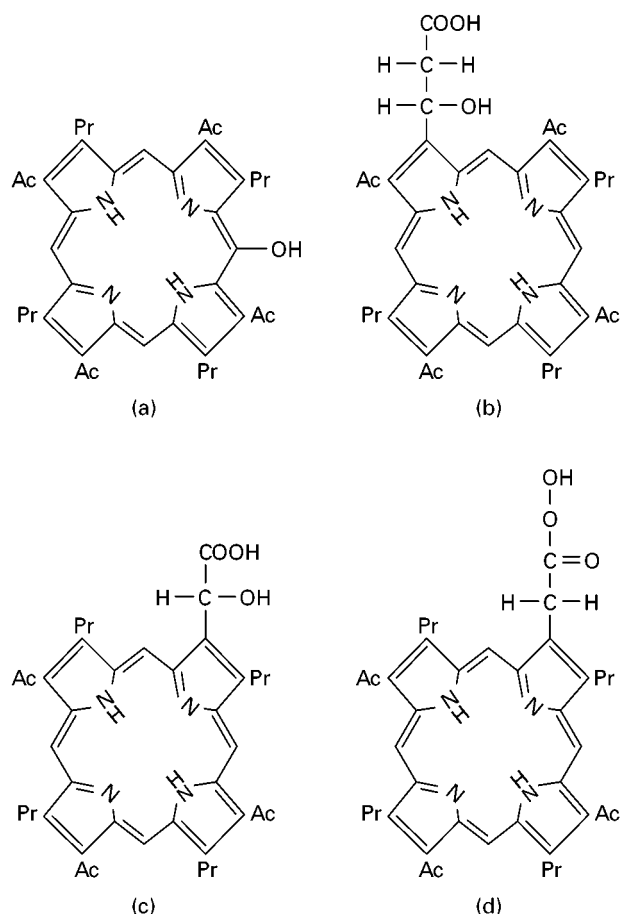


Figure 7 Structures of meso-hydroxyuroporphyrin I (A), β -hydroxypropionic acid uroporphyrin I (B), hydroxyacetic acid uroporphyrin I (C) and peroxyacetic acid uroporphyrin I (D).

elution is carried out by inclusion of 10% (v/v) acetonitrile in each of the gradient solvents, i.e. 1 M ammonium acetate (pH 5.16) and methanol.

Separation of Porphyrin Mixtures by Gradient Elution

The separation of a standard mixture of porphyrins on a C_1 -bonded RP Column (Hypersil-SAS) with the optimized gradient mixtures of 10% acetonitrile in 1 M ammonium acetate, pH 5.16 (solvent A) and 10% acetonitrile in methanol (solvent B) is shown in Figure 4. The complete resolution of uro-, heptacarboxyl-, hexacarboxyl-, pentacarboxyl- and coproporphyrin isomers and the dicarboxyl meso- and proto-porphyrins required just 38 min.

Figure 5 shows the separation of porphyrins on a Hypersil-ODS column, extracted from the faeces of a patient with porphyria cutanea tarda (PCT). It clearly demonstrates the applicability of the system to biomedical analysis.

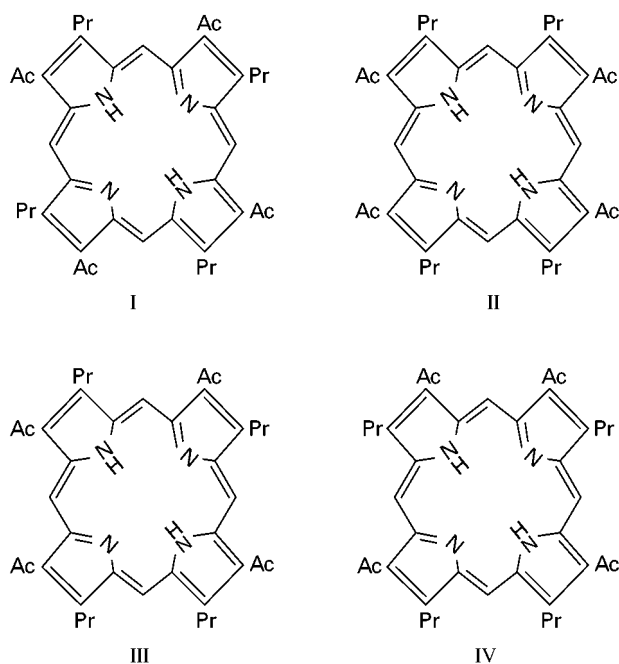


Figure 8 Structures of the four type-isomers of uroporphyrin.

The gradient system can be easily modified if the separation of polar hydroxylated porphyrins is needed. The separation of porphyrins, including hy-

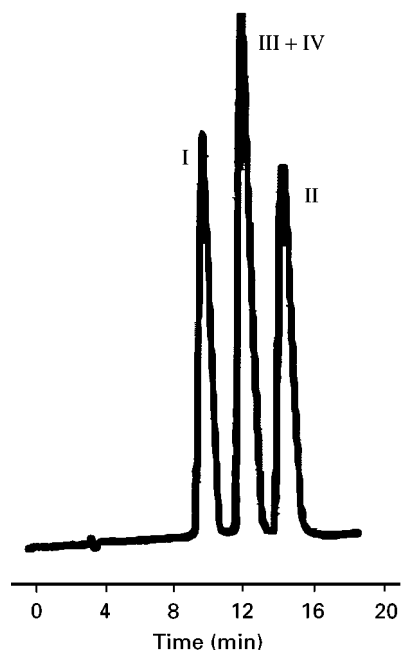


Figure 9 Separation of uroporphyrin type-isomers. Column, Hypersil-ODS (250 \times 4.6 mm, 5- μ m particle size); eluent, 13% (v/v) acetonitrile in 1 M ammonium acetate buffer, pH 5.16; flow rate, 1 mL min⁻¹; detection, 404 nm.

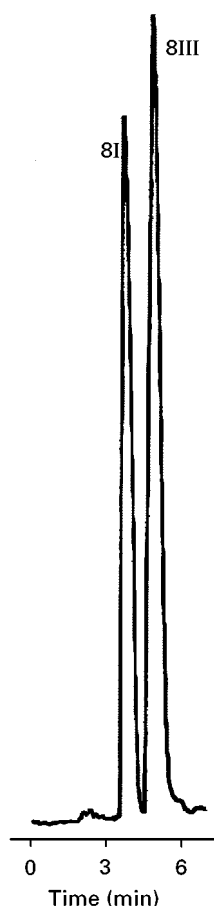


Figure 10 Separation of uroporphyrin I and III isomers. Column, Hypersil-BDS C_{18} (250 \times 4.6 mm, 5- μ m particle size); eluent, 9% (v/v) acetonitrile in 1 M ammonium acetate buffer, pH 5.55; flow rate, 1 mL min^{-1} ; detection, 404 nm.

droxy- and peroxyacid-porphyrins, in the urine of a patient with congenital erythropoietic porphyria (CEP) on a Hypersil-BDS (C_{18}) column with an extended elution programme is shown in **Figure 6**. The structures of the hydroxy- and peroxyacid-porphyrins are shown in **Figure 7**.

Separation of 8-, 7-, 6-, 5- and 4-Carboxylporphyrin Isomers

The separation of the type-isomers, especially type-I and type-III isomers, is of diagnostic value. The separation of isomers of porphyrins resulted from the decarboxylation of uroporphyrinogen I and III is important for understanding the biochemistry of this part of the haem biosynthetic pathway. Individual porphyrin isomers are best separated by isocratic elution with an appropriate amount of acetonitrile or acetonitrile and methanol in 1 M ammonium acetate buffer, pH 5.16, as eluent.

Uroporphyrins (Eight COOH)

There are four type-isomers of uroporphyrin, denoted I, II, III and IV by Fischer to show the four ways in which the acetic acid groups (Ac) and propionic acid groups (Pr) arranged around the eight β -positions of the porphyrin macrocycle (**Figure 8**). The naturally occurring type-I and type-III isomers can be easily separated on an ODS column with 13% (v/v) acetonitrile in 1 M ammonium acetate, pH 5.16, as eluent. The system resolved uroporphyrin I from the III + IV and II isomers but could not separate the III and IV isomers (**Figure 9**). Alternatively, a base-deactivated ODS column (e.g. Hypersil-BDS C_{18}) is used with 9% acetonitrile in 1 M ammonium acetate, pH 5.55, as eluent (**Figure 10**), which provides a more rapid separation of the I and III isomers.

Heptacarboxyl Porphyrins (Seven COOH)

There are five heptacarboxyl porphyrins that can be formed by the decarboxylation of uroporphyrin I and III. Heptacarboxyl porphyrin I (7I; **Figure 11**) is derived from the symmetrical uroporphyrin I and the four type-III heptacarboxyl porphyrins (7a, 7b, 7c and 7d; **Figure 11**) are formed by the random decarboxylation of one of the four acetic acid groups of the asymmetrical uroporphyrin III.

The complete separation of the four type-III heptacarboxyl porphyrins has not been achieved, although the type-I isomer was easily separated from the type-III isomers. With 28% acetonitrile-methanol (1 : 9 v/v) in 1 M ammonium acetate (pH 5.16) as eluent on a Hypersil-BDS column, the four type-III isomers were resolved into three peaks in the elution order 7c, 7d and 7a + 7b (**Figure 12**). The four type-III isomers could, however, be completely separated following conversion to the corresponding heptacarboxyl porphyrinogens by reduction (see section on Reversed-Phase Chromatography of Porphyrinogens).

Hexacarboxyl Porphyrins (Six COOH)

The structures of the two type-I (6Iab and 6Iac) and six type-III (6ab, 6ac, 6ad, 6bc, 6bd and 6cd) hexacarboxyl porphyrin isomers are shown in **Figure 13**. On an ODS column (Hypersil-ODS) with 16% (v/v) acetonitrile in 1 M ammonium acetate, pH 5.16 as mobile phase, the two type-I isomers were well resolved from the most abundant naturally occurring 6ad, but complete separation of the other isomers was not achieved (**Figure 14**).

Pentacarboxyl Porphyrins (Five COOH)

There are four type-III (5bcd, 5acd, 5abc and 5abd) and one type-I (5I) pentacarboxyl porphyrins (**Figure 15**). These five isomers have been separated on

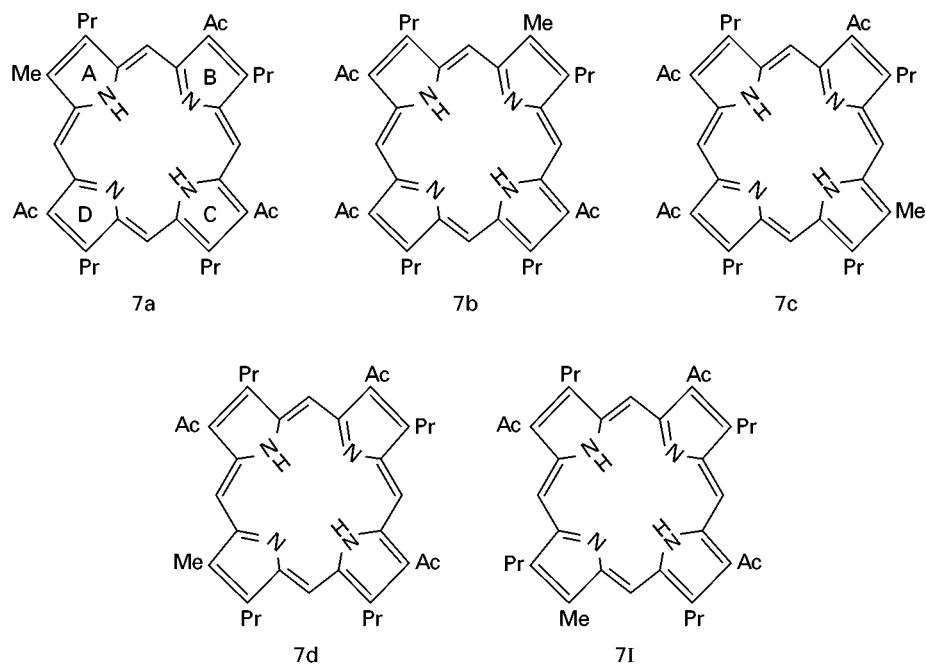


Figure 11 Structures of heptacarboxyl porphyrin isomers. Isomer 7I is heptacarboxyl porphyrin I. Isomers 7a, 7b, 7c and 7d are type-III isomers. The letters a, b, c and d denote the position of methyl group (Me), i.e. the position in which an acetic acid group (Ac) has been decarboxylated. Pr represents a propionic acid group.

a Hypersil-BDS column with acetonitrile–methanol–1 M ammonium acetate buffer (4.5 : 40.5 : 55, by volume), pH 5.16, as eluent (Figure 16). The elution order was 5I, 5bcd, 5abc, 5acd, and 5abd.

Coproporphyrins (Four COOH)

The structures of the four type-isomers (I, II, III and IV) of coproporphyrin are shown in Figure 17. All

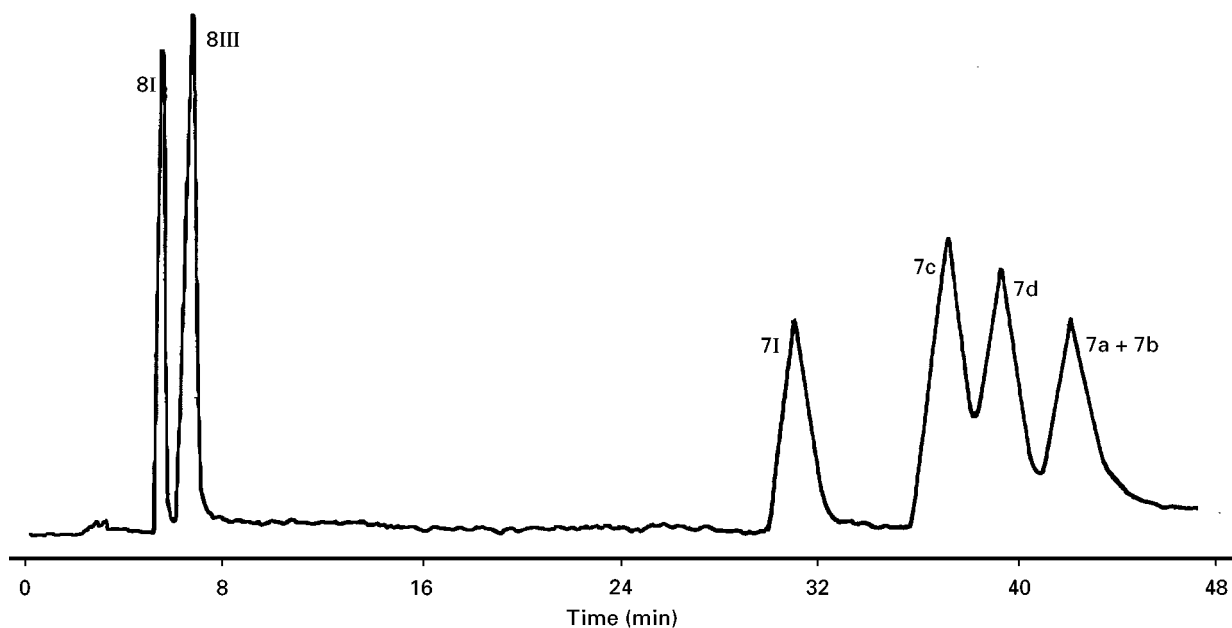


Figure 12 Separation of heptacarboxyl porphyrin isomers. Column, Hypersil-ODS (250 × 4.6 mm, 5- μ m particle size); eluent, 28% (v/v) acetonitrile–methanol (1 : 9) in 1 M ammonium acetate buffer, pH 5.16; flow rate, 1 mL min⁻¹; detection, 404 nm. See Figure 11 for structures and peak identification.

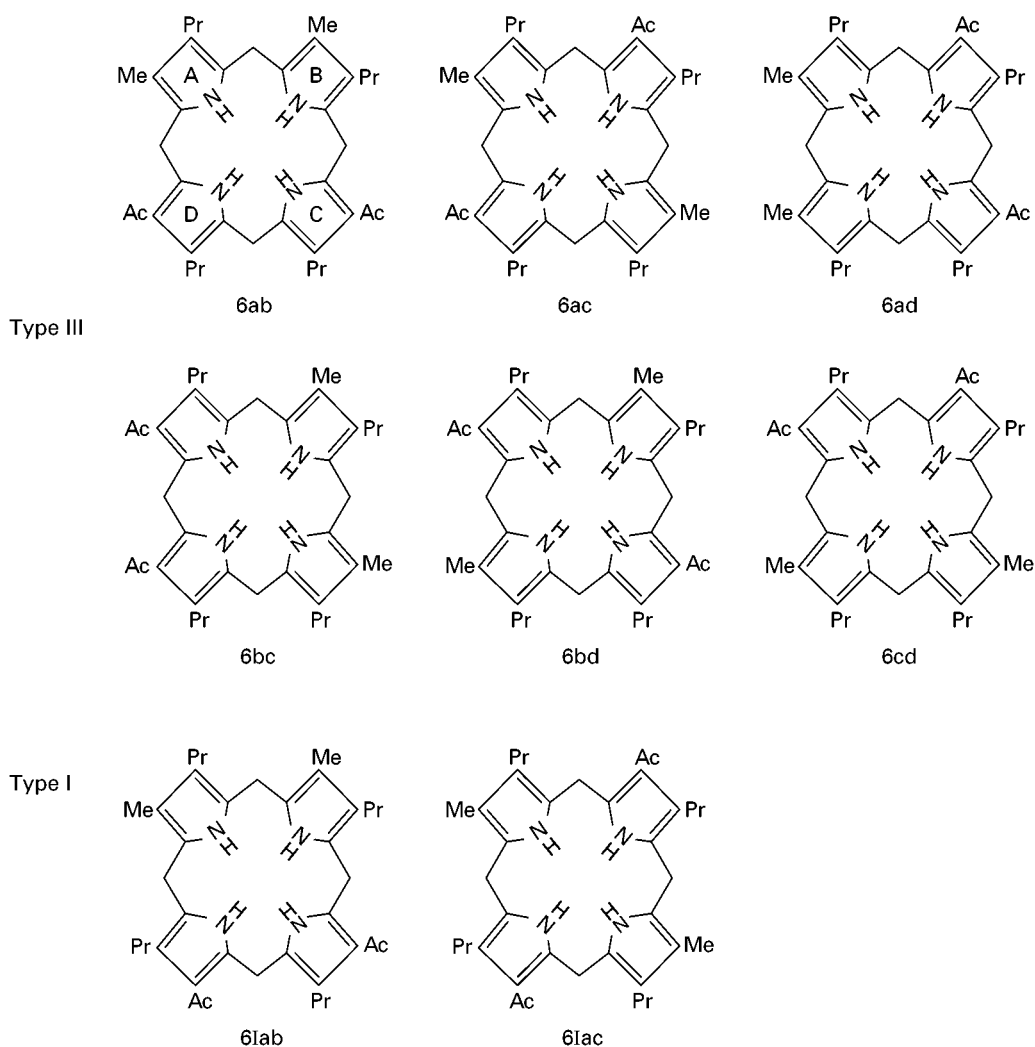


Figure 13 Structures of hexacarboxyl porphyrin isomers. 6lab and 6lac are type-I and 6ab, 6ac, 6ad, 6bc, 6bd and 6cd are type-III isomers. The letters a, b, c and d denote the position of methyl groups.

four isomers were easily separated by reversed-phase HPLC on an ODS column with 26% (v/v) acetonitrile in 1 M ammonium acetate buffer (pH 5.16) as eluent (Figure 18). Rapid separation of coproporphyrin I and III isomers could be achieved by using a mobile phase of 30% acetonitrile in 1 M ammonium acetate buffer (pH 5.16) or employing a Hypersil-BDS column which is less retentive but still maintains the resolution.

Retention Mechanism of Porphyrins in Reversed-Phase Chromatography

The dominant retention mechanism is hydrophobic interaction between the porphyrin side-chain substituents and the non-polar hydrocarbonaceous functions of the stationary phase surface. The relative hydrophobicity of the side-chain β -substituents

of the porphyrins is $\text{CH}=\text{CH}_2 > \text{CH}_2\text{CH}_3 > \text{CH}_3 > \text{CH}_2\text{CH}_2\text{COOH} > \text{CH}_2\text{COOH}$. The relative retention of the porphyrins is therefore dependent on the relative number of hydrophobic substituents available for interaction and is thus dominated by the number of alkyl (particularly methyl) groups present in the molecule. The retention increases with increasing number of alkyl substituents, and the following elution order was observed; uroporphyrin (8COOH), heptacarboxyl porphyrin (7COOH, 1CH₃), hexacarboxyl porphyrin (6COOH, 2CH₃), pentacarboxyl porphyrin (5COOH, 3CH₃), coproporphyrin (4COOH, 4CH₃), mesoporphyrin (2COOH, 4CH₃, 2CH₂CH₃) and protoporphyrin (2COOH, 4CH₃, 2CH=CH₂).

This retention mechanism is also applicable to the separation of type-isomers. For example, the elution order (I, III, IV, II) of coproporphyrin isomers could be explained as follows.

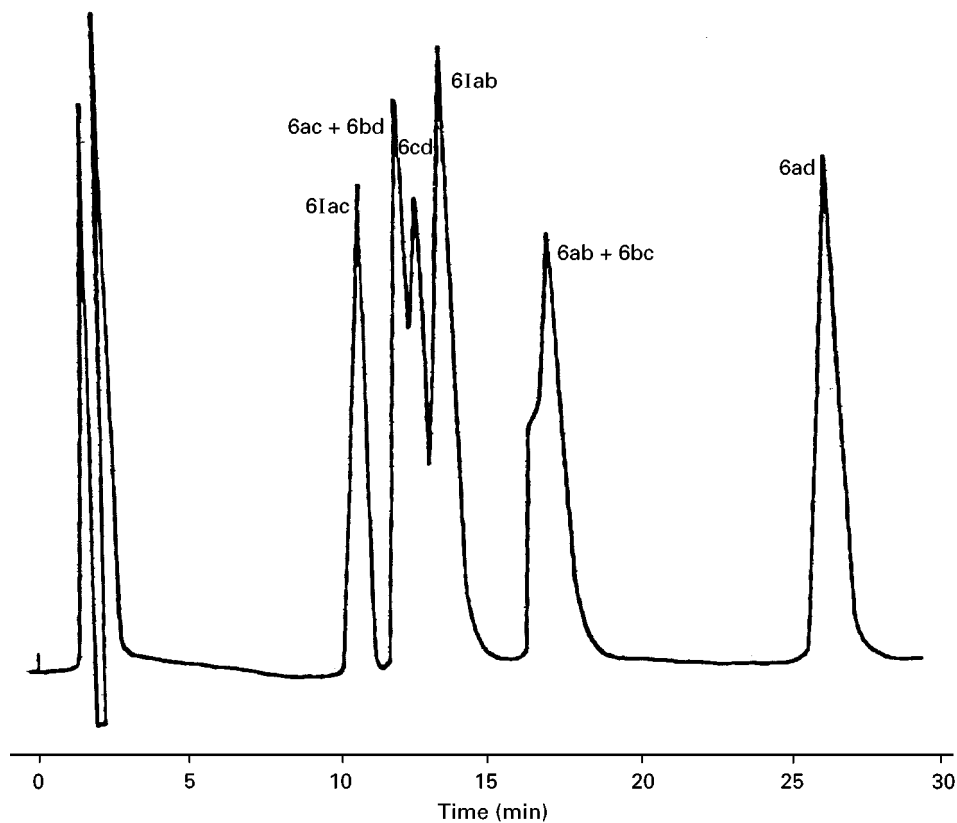


Figure 14 Separation of hexacarboxyl porphyrin isomers. Column, Hypersil-ODS (250 × 4.6 mm, 5- μ m particle size); eluent, 16% (v/v) acetonitrile in 1 M ammonium acetate buffer, pH 5.16; flow rate, 1 mL min⁻¹; detection, 404 nm. See Figure 13 for structures and peak identification. (Reproduced from Lim *et al.* (1983) *Journal of Chromatography* 282: 629–641, with permission from Elsevier Science.)

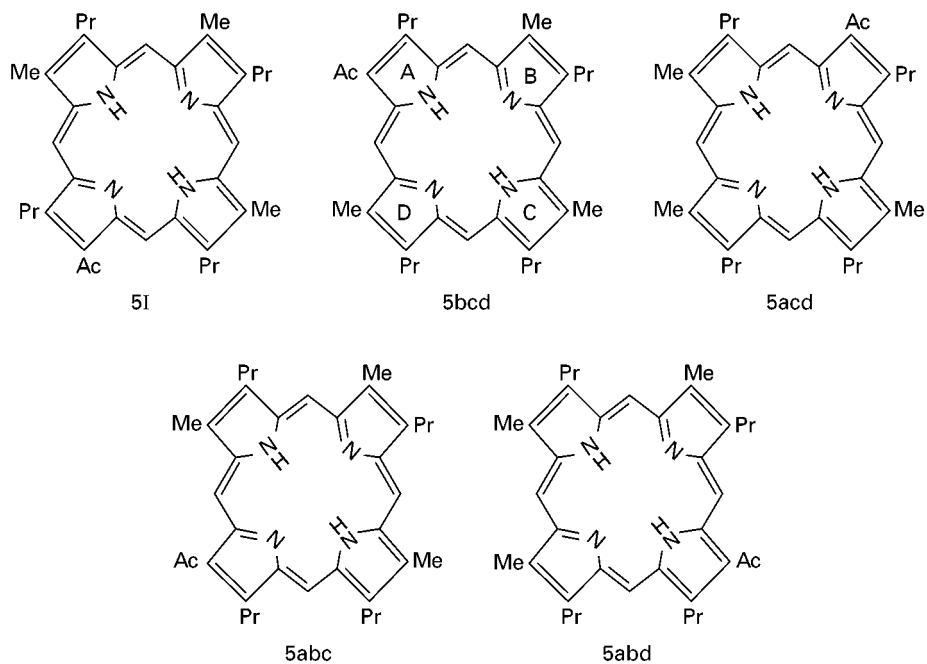


Figure 15 Structures of pentacarboxyl porphyrin isomers. 5I is type-I pentacarboxyl porphyrin. Isomers 5bcd, 5acd, 5abc and 5abd are type-III isomers. The letters a, b, c and d denote the position of methyl groups.

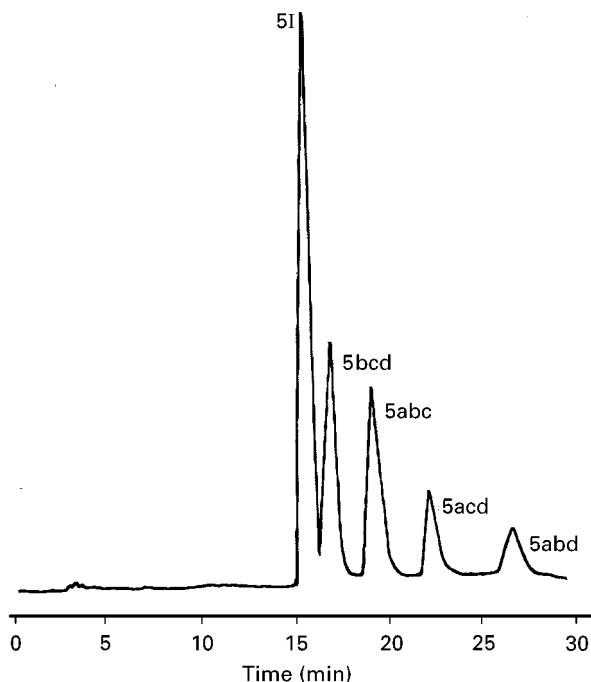


Figure 16 Separation of pentacarboxyl porphyrin isomers. Column, Hypersil-BDS C_{18} (250×4.6 mm, $5\text{-}\mu\text{m}$ particle size); eluent, acetonitrile-methanol-1 M ammonium acetate buffer (4.5 : 40.5 : 55, by volume), pH 5.16; flow rate, 1 mL min^{-1} ; detection, 404 nm. See Figure 15 for structures and peak identification.

Coproporphyrin II is the longest retained compound because it has two pairs of adjacent CH_3 groups (Figure 17) which provides the largest hydro-

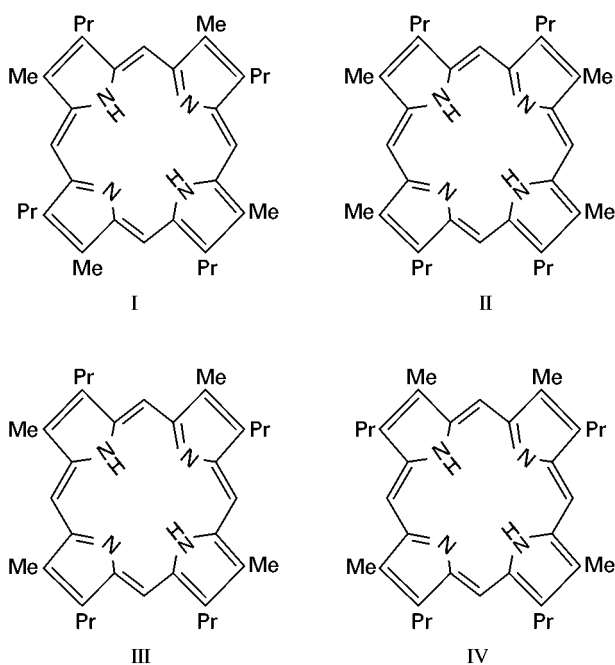


Figure 17 Structures of type-I, II, III and IV isomers of coproporphyrin.

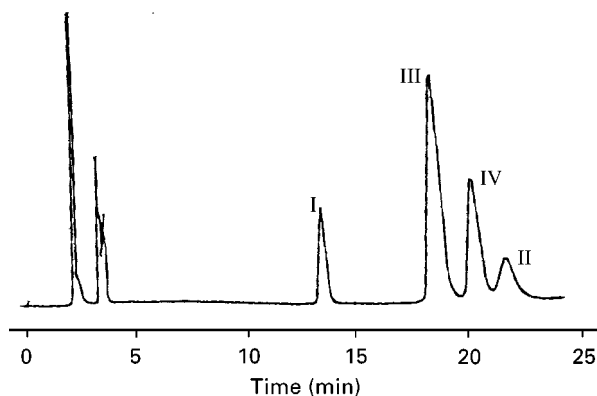


Figure 18 Separation of type-I, II, III and IV isomers of coproporphyrin. Column, Hypersil-ODS (250×4.6 mm, $5\text{-}\mu\text{m}$ particle size); eluent, 26% (v/v) acetonitrile in 1 M ammonium acetate buffer, pH 5.16; flow rate, 2 mL min^{-1} ; detection, 404 nm.

phobic surface area available for interaction. The symmetrical coproporphyrin I has no adjacent CH_3 groups and is the least hydrophobic. It is the fastest eluting isomer. Coproporphyrin III and IV each have a pair of adjacent CH_3 groups. In this situation the relative distance between the adjacent CH_3 pair and the remaining two non-adjacent CH_3 groups becomes an important factor in determining the relative hydrophobicity. In coproporphyrin IV, each of the adjacent CH_3 groups is five bonds away from the nearest

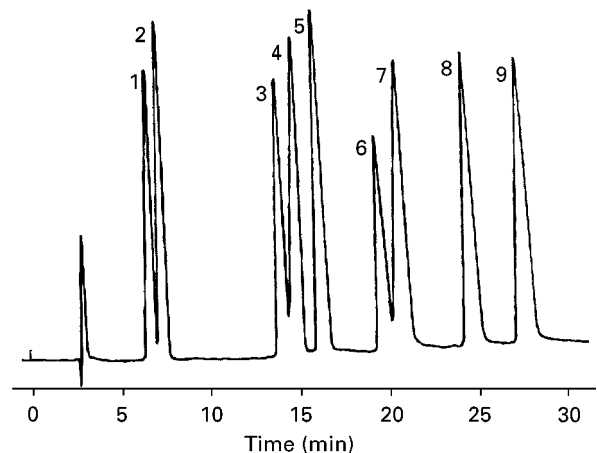


Figure 19 Separation of dicarboxylic porphyrins and metalloporphyrins. Column, Hypersil-SAS (C_8 , 250×4.6 mm, $5\text{-}\mu\text{m}$ particle size); eluent, methanol (solvent A) and 1 M ammonium acetate buffer, pH 4.6 (solvent B); elution, 62% A isocratically for 6 min, then linear gradient to 70% A from 6.1 to 13 min followed by isocratic elution at 75% A; flow rate, 1 mL min^{-1} ; detection, 404 nm. Peaks: 1 = Co(proto porphyrin); 2 = Co(mesoporphyrin); 3 = Fe(proto); 4 = Fe(meso); 5 = deuteroporphyrin; 6 = Zn(meso); 7 = Zn(proto); 8 = mesoporphyrin; 9 = protoporphyrin. (Reproduced with permission from Lim *et al.* (1984) *Journal of Chromatography* 317: 333-341.)

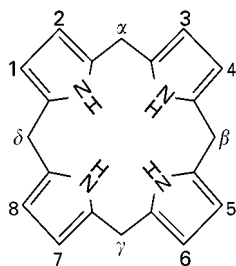


Figure 20 Structure of porphyrinogen (hexahydroporphyrin) macrocycle.

non-adjacent CH_3 group. In coproporphyrin III these are five and six bonds apart, respectively. The slightly longer distance (one bond-distance) between one of the adjacent CH_3 groups and its nearest non-adjacent CH_3 group (six instead of five bonds apart) is sufficient to make coproporphyrin III less hydrophobic than and therefore eluted before coproporphyrin IV (Figure 18).

The elution order of the penta- and hexa-carboxyl porphyrin isomers could be similarly predicted. This also explains why it was difficult to resolve the type-III heptacarboxyl porphyrin isomers since the single CH_3 group present in these molecules makes them very similar in hydrophobic surface area. The study of retention behaviour is useful in elucidating the nature of side-chain substituents present in unknown porphyrins.

Reversed-Phase Chromatography of Metalloporphyrins

The most important naturally occurring metalloporphyrins are the Mg, Fe, Cu, Zn and Co complexes of dicarboxyl porphyrins. Iron complexes form the prosthetic groups of the various haemoproteins, Mg complexes are found in the chlorophylls and Co complex in vitamin B_{12} . In heavy metal poisoning, particularly lead intoxication, erythrocyte Zn-protoporphyrin is elevated.

The mobile phases developed for the separation of porphyrins have been modified for the separation of dicarboxyl porphyrins and metalloporphyrins. These highly hydrophobic porphyrins are best separated on the least hydrophobic C_1 -bonded column. Methanol is the preferred organic modifier since the dicarboxyl porphyrins and their metal complexes do not form extensive hydrogen bonds with the methanol extracted into the stationary phase, as with uroporphyrin. Methanol gave better resolution of dicarboxyl porphyrins and their metal complexes and is totally miscible with the 1 M ammonium acetate buffer (pH 4.6) used in the mobile phase. The separation of

a mixture of dicarboxyl porphyrins and metalloporphyrin is shown in Figure 19.

The insertion of a metal ion which completely occupies the centre of the porphyrin hole significantly alters the electronic environment around the central nitrogen atoms. The retention of the metalloporphyrin is therefore dependent on the ability of the inserted metal ion to accept axial ligands from the mobile phase. Co and Fe complexes are good axial ligand acceptors and may add two extra ligands; Zn complex can add one extra ligand, while further coordination of the Cu complex is only possible under special conditions. The addition of polar axial ligands leads to a decrease in the overall hydrophobicity of a molecule and therefore its retention. Thus, the elution order of Co, Fe, Zn and Cu complexes, was observed for both meso- and proto-porphyrins.

The elution order of the Zn and Cu complexes of meso- and proto-porphyrins is the same as that for meso- and proto-porphyrins with the former eluted before the latter. These metalloporphyrins do not accept axial ligands readily and their relative reten-

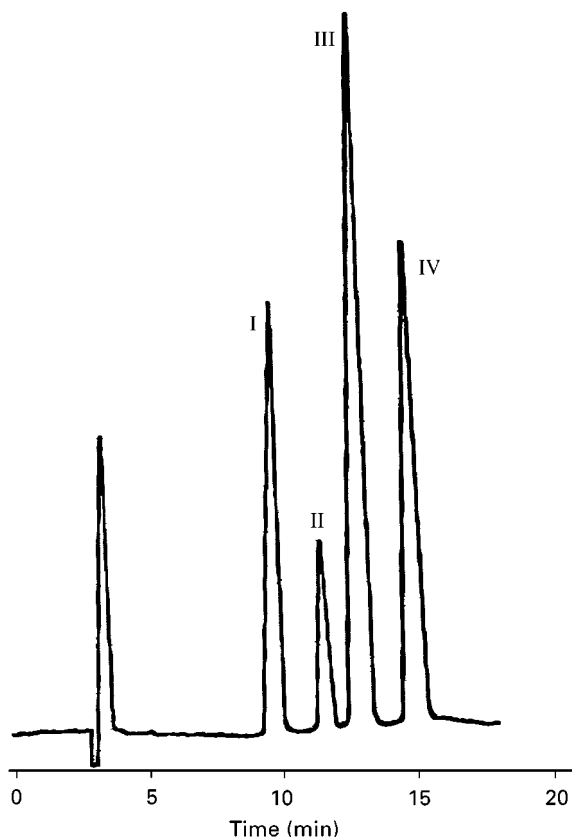


Figure 21 Separation of coproporphyrinogen I, II, III and IV isomers. Column, Hypersil-ODS (250 × 4.6 mm, 5- μm particle size); eluent, 25% (v/v) acetonitrile in 1 M ammonium acetate buffer, pH 5.16; flow rate, 1 mL min^{-1} ; detection, amperometric at +0.75 V. (Reproduced with permission from Lim *et al.* (1986) *Biochemistry Journal* 234: 629–633.)

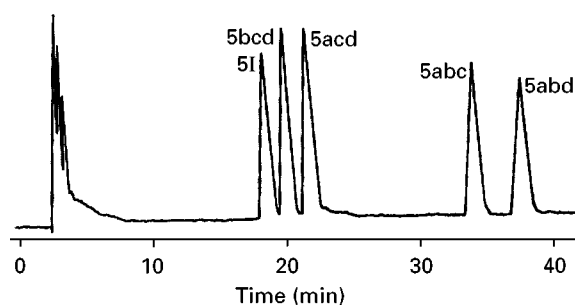


Figure 22 Separation of pentacarboxyl porphyrinogen isomers. Column, Hypersil-ODS (250 × 4.6 mm, 5- μ m particle size); eluent, 40% (v/v) methanol in 1 M ammonium acetate buffer, pH 5.16; flow rate, 1 mL min⁻¹; detection, amperometric at +0.70 V.

tion is still governed by the relative hydrophobicity of the side-chain substituents.

The elution order of the Co and Fe complexes of meso- and proto-porphyrins is the reverse of that observed for Zn and Cu complexes. Co and Fe complexes are excellent axial ligand acceptors. The decrease in electron density at the pyrrolic nitrogens in metalloprotoporphyrins due to the vinyl groups of protoporphyrin is reflected in the chelated metals, leading to increased affinity for the donor electrons of the extra axial ligands. This leads to a decrease in the hydrophobicity of Co- and Fe-protoporphyrins.

Reversed-Phase Chromatography of Porphyrinogens

The porphyrinogens are hexahydroporphyrins (Figure 20). They are the true intermediates in the bio-

synthesis of haem, chlorophylls and vitamin B₁₂. Porphyrinogens are not often separated because they are easily oxidized to the corresponding porphyrins by air and it is mainly the porphyrins which are present in body fluids and excreta. Studies have shown that isomers of porphyrinogens are better resolved than the corresponding porphyrins. The separation of porphyrinogen isomers is therefore important in situation where the separation of porphyrin isomers is incomplete or could not be achieved.

Coproporphyrinogen, Penta-, Hexa-, Hepta-carboxyl Porphyrinogens and Uroporphyrinogen Isomers

The complete separation of coproporphyrinogen I, II, III and IV isomers could be achieved in 15 min on an ODS column with 25% (v/v) acetonitrile in 1 M ammonium acetate buffer (pH 5.16) as mobile phase (Figure 21). Porphyrinogens are more flexible compounds than the rigid porphyrin macrocycles. In the flexible coproporphyrinogen molecules, the small CH₃ substituents in each isomers may be subjected to varying degrees of steric hindrance or shielding by the larger propionic acid groups, depending on the adopted conformation. This alters the expected available surface area for hydrophobic interaction and makes prediction of elution order based on hydrophobic interaction by the methyl group difficult. The conformation of porphyrinogens under reversed-phase conditions have not been studied.

The superior separation of porphyrinogens compared with porphyrins was similarly observed for penta-, hexa- and hepta-carboxyl porphyrinogens

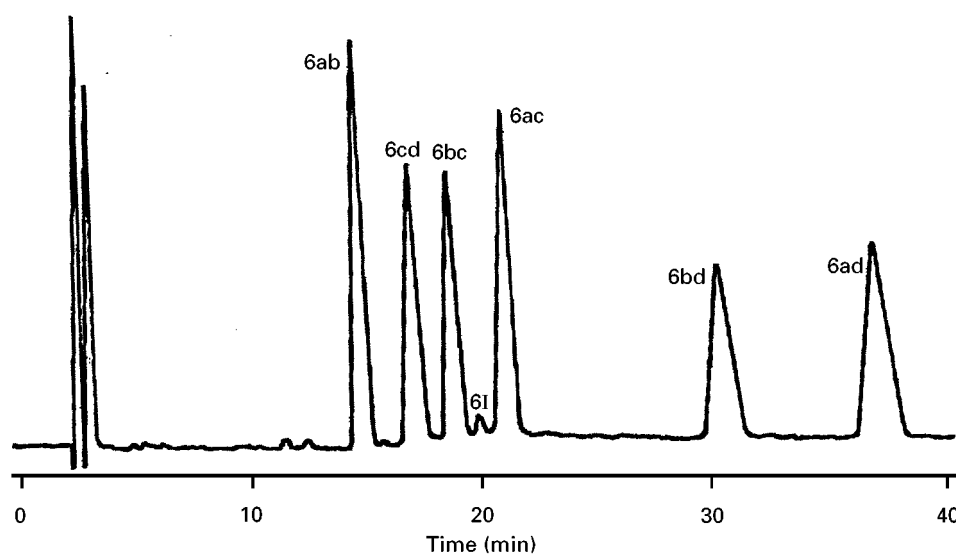


Figure 23 Separation of hexacarboxyl porphyrinogen isomers. Column, Hypersil-ODS (250 × 4.6 mm, 5- μ m particle size); eluent, acetonitrile-methanol-1 M ammonium acetate (8 : 12 : 80, by volume); pH 5.16; flow rate, 1 mL min⁻¹; detection, amperometric at +0.70 V.

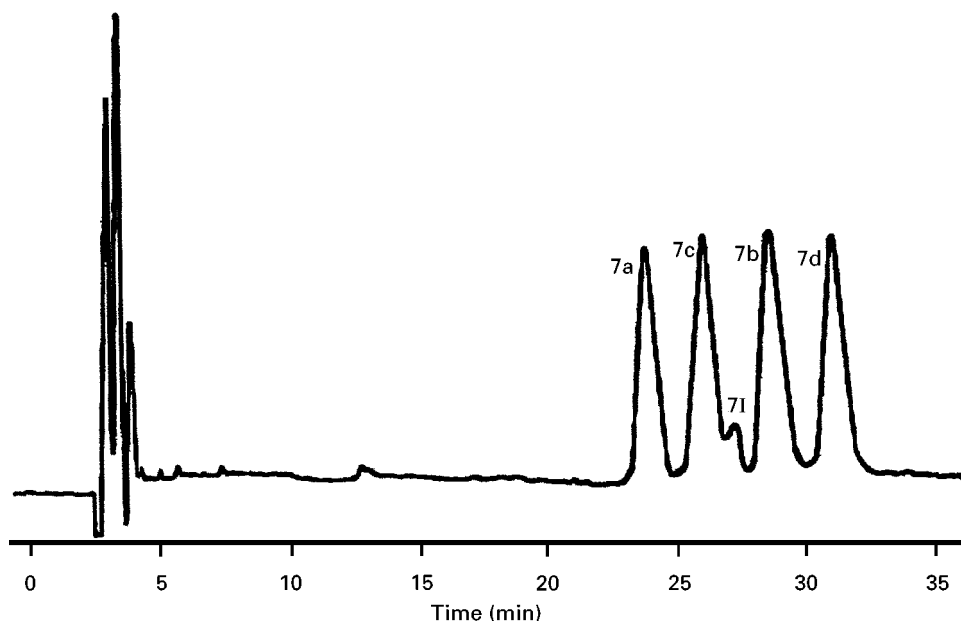


Figure 24 Separation of heptacarboxyl porphyrinogen isomers. Column, Hypersil-ODS (250×4.6 mm, $5\text{-}\mu\text{m}$ particle size); eluent, acetonitrile–methanol–1 M ammonium acetate, (7 : 3 : 90, by volume) pH 5.16; flow rate, 1 mL min^{-1} ; detection, amperometric at $+0.70\text{ V}$. (Reproduced with permission from Lim *et al.* (1987) *Biochemistry Journal* 247: 229–232.)

(Figures 22, 23 and 24, respectively). The improvement for the heptacarboxyl porphyrinogens was such that all four type-III isomers could be easily resolved (Figure 24).

For the uroporphyrinogens, there was no improvement in resolution over the porphyrins and a reversal of elution order was observed for the type-I and type-III isomers (Figure 25).

Detectors for Porphyrins and Porphyrinogens

Porphyrins have intense red fluorescence and are therefore easily detected with great sensitivity and specificity with a fluorescence detector set at excitation wavelengths of 400–420 nm and emission wavelengths of 600–620 nm.

Porphyrins have an intense absorption band at about 400 nm (Soret band) with molar extinction coefficients often around 400 000. Detection at the Soret band region with a UV-visible detector also provides excellent detectability.

Porphyrinogens are colourless compounds devoid of fluorescence and with only weak UV absorptions at the 220 nm region. They are best detected electrochemically by the oxidation mode because of the ease of oxidation of these compounds.

In terms of sensitivity and specificity, the mass spectrometer is the ‘detector’ of choice. Online LC–MS, especially with electrospray quadrupole

time-of-flight MS–MS, allows porphyrins, metalloporphyrins and porphyrinogens to be detected and characterized with ease.

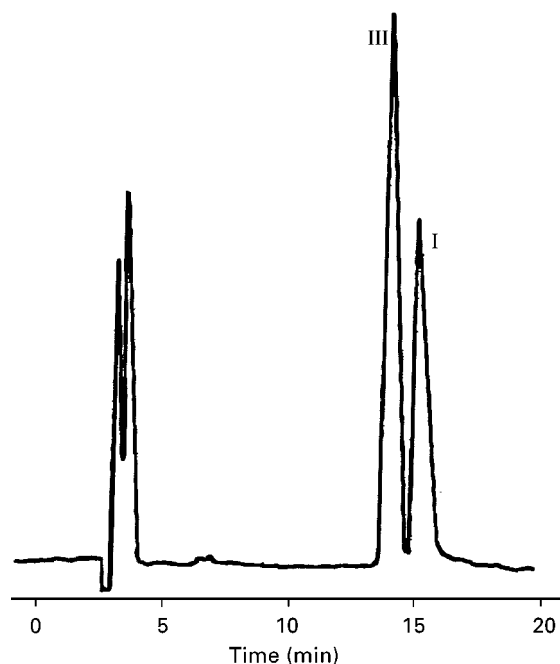


Figure 25 Separation of uroporphyrinogen I and III isomers. Column, Hypersil-ODS (250×4.6 mm, $5\text{-}\mu\text{m}$ particle size); eluent, 6% (v/v) acetonitrile in 1 M ammonium acetate buffer, pH 5.16; flow rate, 1 mL min^{-1} ; detection, amperometric at $+0.70\text{ V}$.

Future Developments

There are two areas in porphyrin separation which are expected to develop further in the future. The first is in column technology. The improvement achieved by the introduction of base-deactivated reversed-phase is expected to continue and better columns with improved resolution and reproducibility can be expected. The second is in online LC-MS-MS operation. With the introduction of high sensitivity and resolution mass spectrometers, analysis of porphyrins will be a lot easier in the future.

See also: II/Chromatography: Liquid: Detectors: Mass Spectrometry.

Further Reading

Dolphin D (ed.) (1978) *The Porphyrins*, vol. 1. New York: Academic Press.

Jordan PM (ed.) (1991) *Biosynthesis of Tetrapyrroles*. London: Elsevier.

Li F, Lim CK and Peters TJ (1987) HPLC of porphyrinogens with electrochemical detection. *Chromatographia* 24: 421-422.

Lim CK, Rideout JM and Peters TJ (1984) High-performance liquid chromatography of dicarboxylic porphyrins and metalloporphyrins: retention behaviour and biomedical applications. *Journal of Chromatography* 317: 333-341.

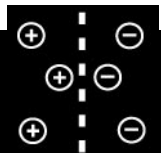
Lim CK, Li F and Peters TJ (1988) High-performance liquid chromatography of porphyrins. *Journal of Chromatography, Biomedical Applications* 429: 123-153.

Luo J and Lim CK (1995) Isolation and characterization of new porphyrin metabolites in human porphyria cutanea tarda and in rats treated with hexachlorobenzene by HPTLC, HPLC and liquid secondary ion mass spectrometry. *Biomedical Chromatography* 9: 113-122.

Moss GP (1987) Nomenclature of tetrapyrroles. *Pure and Applied Chemistry* 59: 779-832.

Smith KM (ed.) (1974) *Porphyrins and Metalloporphyrins*. Amsterdam: Elsevier.

POWDERED RESINS: CONTINUOUS ION EXCHANGE



P. A. Yarnell, Graver Technologies, Glasgow, DE, USA

Copyright © 2000 Academic Press

Introduction

The use of finely divided (powdered) forms of ion exchange resins began in the early 1960s. Prior to that, synthetic ion exchange resins were manufactured as granules, or preferably spherical beads. The ion exchange granules and beads were used in packed beds to treat liquids, most commonly water. The Graver Water Conditioning Company pioneered the use of the powdered ion exchange resins made by grinding ion exchange resin beads or granules into powders. They discovered that a thin layer of powdered resin offered a dramatic improvement in ion exchange reaction rate versus a conventional packed bed of resin. In 1966 Joseph A. Levendusky of Graver Water Conditioning patented a powdered resin system (named Powdex®) that has been the basis for most practical applications of this technology. This process utilized a pre-coat of powdered ion exchange resins applied to a septum or filter. Thus, the pre-coat

process incorporated ion exchange and filtration into one unit operation.

Basic Principles

The original pre-coats were made by combining powdered anion exchange resin with powdered cation exchange resin in a water slurry. Both types of resin were ground moist (40-60% moisture content) into powders using grinding equipment such as hammer mills. This grinding process resulted in a distribution of particle sizes, typically from 1 to 200 µm in diameter. These distributions were centred in the 35-70 µm range. Thus, the powdered ion exchange particles are roughly two orders of magnitude smaller than conventional ion exchange resins (Figure 1). The grinding process also results in a tremendous increase in surface area and, consequently, a higher surface area to weight ratio.

Particle size of powdered ion exchange resins is the most important factor in determining performance of pre-coats. In these applications, resin particle size influences ion exchange capacity utilization, filtration efficiency, filtration capacity and pre-coat characteristics (integrity, uniformity, lifetime). In their classic paper, Frisch and Kunin elucidated the effects of